



**Prediction of high-temperature superconductivity in  $C2/c-24$  solid hydrogen**Mehmet Dogan , Sehoon Oh , and Marvin L. Cohen <sup>\*</sup>*Department of Physics, University of California, Berkeley, California 94720, USA  
and Materials Sciences Division, Lawrence Berkeley National Laboratory, Berkeley, California 94720, USA* (Received 16 July 2021; revised 22 December 2021; accepted 19 January 2022; published 31 January 2022)

Recent experimental developments in hydrogen-rich materials at high pressures have put this class of materials above others in the race toward room-temperature superconductivity. As it is the basis of all the materials in this class, the efforts to determine the properties of pure solid hydrogen at high pressures remain intense. Most notably, a recent experimental study of the metallization of hydrogen identified the crystal phase of the solid as the  $C2/c-24$  molecular phase up to  $\sim 425$  GPa [Loubeyre *et al.*, *Nature (London)* **577**, 631 (2020)]. It is possible that the observed metallization is caused by band structure effects and not a structural phase transition, and the material remains in this crystal phase up to higher pressures [Dogan *et al.*, *J. Phys.: Condens. Matter* **33**, 03LT01 (2020)]. Therefore, it is of crucial importance to determine the superconducting properties of the  $C2/c-24$  phase. Here, we employ a Wannier function-based dense  $k$ -point and  $q$ -point sampling to compute the electron-phonon coupling and superconducting properties of molecular hydrogen in the  $C2/c-24$  phase. We find that the material has a high superconducting transition temperature of 242 K at 500 GPa. We also find that the transition temperature rapidly increases with pressure in the 400–500-GPa range.

DOI: [10.1103/PhysRevB.105.L020509](https://doi.org/10.1103/PhysRevB.105.L020509)

Hydrogen was predicted to transition to an atomic crystal and a metal in its solid form in 1935 [1], which was followed by the prediction that it would have a high superconducting transition temperature in 1968 [2]. However, determining the transition to the atomic phase as well as predicting the crystal structure of the molecular phase of solid hydrogen was elusive for several decades until the early 2000s, when a collection of candidates was discovered [3–6]. In the following two decades, through the increasingly sophisticated computational methods and steadily improving experimental studies, the leading candidates emerged as the three molecular phases ( $C2/c-24$ ,  $Cmca-12$ ,  $Cmca-4$ ) and one atomic phase ( $I4_1/amd-2$ ) (number after the dash denotes the number of atoms in the unit cell) [7–16]. As the pressure increases, hydrogen may metallize either via the closure of the band gap in a molecular phase or a structural phase transition into a different molecular phase (whose gap is already closed at that pressure) or an atomic phase. Computational studies have not definitively shown which of these scenarios should occur and at which pressure beyond the consensus that several phases become competitive in the 300–500-GPa range. The reason is that hydrogen nuclei are too light for the common static nuclei approximation to be accurate, and different sets of phase transitions are predicted when different methodologies of accounting for the quantum nature of the nuclei are used.

Because of the developments in the diamond-anvil cell technology, the accessible pressure range gradually reached 400 GPa in the 2000s and 2010s, resulting first in the observation of black hydrogen (a semiconductor with a direct gap below the visible range) around 310–320 GPa [17–20],

and second in the observation of increased conductivity around 350–360 GPa, where solid hydrogen might become semimetallic [21,22]. Recently, an experiment by Loubeyre *et al.* [23] employed infrared (IR) absorption measurements to track the vibron frequency and the direct electronic band gap with pressure up to 425 GPa. In this experiment, it was observed that the IR-active vibron frequency linearly decreases with pressure from 150 to 425 GPa, which indicates that there is likely no phase transition in this pressure range. At the same time, the direct band gap gradually decreases between 360–420 GPa, but abruptly drops below the minimum experimentally available value of  $\sim 0.1$  eV. Although there are important methodological disagreements between different experimental groups [24–26], there is general agreement that some kind of band-gap closure occurs in the 425–440-GPa range, as also indicated by the abrupt saturation of IR absorption around 425 GPa observed by Dias *et al.* [21] and similar measurements in the Raman spectra around 440 GPa by Eremets *et al.* [22]. Finally, it is possible that a phase transition to atomic metallic hydrogen occurs around 500 GPa [27,28].

In a previous work [29], we showed that the vibron frequencies of the  $C2/c-24$  phase calculated in the anharmonic regime match well with the observations of Loubeyre *et al.* [23] up to 425 GPa. We also demonstrated that it is possible to interpret the observed changes in the direct band gap as a series of pressure-induced changes in the band structure without the need to postulate a structural phase transition. Hence, it is possible that the material remains in the  $C2/c-24$  phase at higher pressures, potentially up to 500 GPa. Although the atomic and electronic structures of this phase have been reported previously [5,11,29], due to its 24-atom unit cell, its superconducting properties have remained elusive. However,

<sup>\*</sup>mlcohen@berkeley.edu

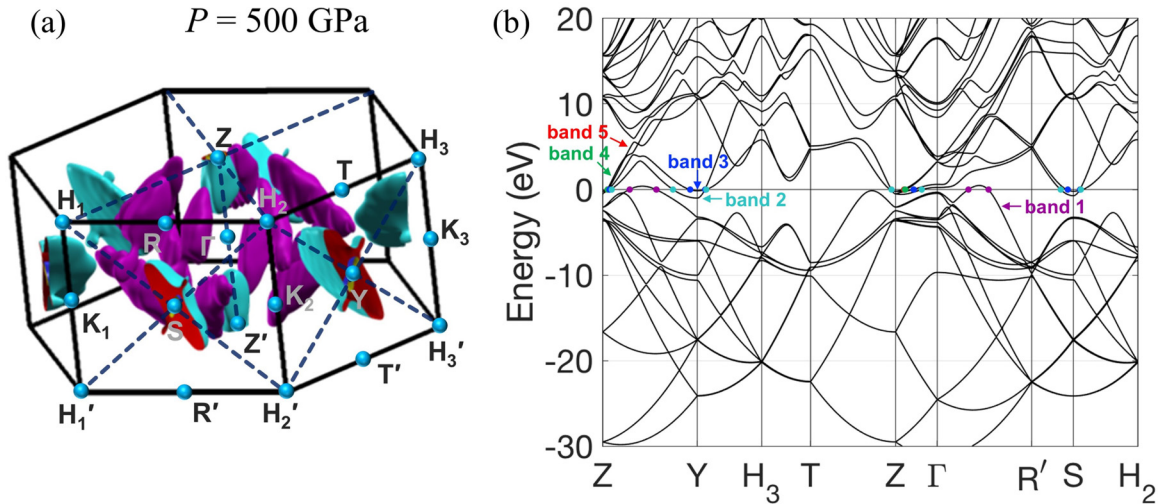


FIG. 1. Fermi surface and band structure at 500 GPa. (a) The first Brillouin zone and the Fermi surface of the  $C2/c-24$  phase of hydrogen at 500 GPa pressure, with high-symmetry points labeled. (b) Band structure of the  $C2/c-24$  phase of hydrogen at 500-GPa pressure. Energies are relative to the Fermi energy. The bands that cross the Fermi energy are pointed out and the band crossings are labeled with filled circles. The colors of these labels match the outer surface colors of the Fermi surface sheets in (a).

with all the recent developments in hydrogen-rich materials at high pressures that are approaching room-temperature superconductivity [30–34], it is even more crucial to understand the superconductivity of this pure hydrogen structure.

Here, we investigate the electronic structure, vibrational properties, electron-phonon coupling, and superconducting properties of molecular hydrogen in the  $C2/c-24$  phase at 400, 450, and 500 GPa using density-functional theory calculations in the generalized gradient approximation, anharmonic corrections with the self-consistent phonon approach, and a Wannier function-based dense  $k$ -point and  $q$ -point sampling (see the Supplemental Material for details [35], and Refs. [36–45] therein).

The atomic structure of the  $C2/c-24$  phase is shown in Fig. S1, which consists of van der Waals-bonded layers of molecular hydrogen. The distorted hexagonal unit cell consists of 24 atoms where 6 atoms (3 molecules) lie in 4 inequivalent planes. The Fermi surface and the band structure for 400 and 450 GPa are shown in Fig. S2 and Fig. S3, respectively. As pressure increases, the material first transitions from a semiconductor to semimetal with a valence band (band 1) and a conduction band (band 2) crossing the Fermi energy (Fig. S2). As the pressure increases, the Fermi surface consisting of the band 1 and band 2 sheets grows, and other bands start crossing the Fermi energy in the vicinity of the  $Z$  point (Fig. S3). At 500 GPa, the Fermi surface consists of many electron and hole pockets and with five bands crossing the Fermi energy at various points in the Brillouin zone, as shown in Fig. 1. The density of states at the Fermi energy is 0.002, 0.010, and 0.022 states/eV/atom for 400, 450, and 500 GPa, respectively.

We note here that we use the generalized gradient approximation which underestimates band gaps. A more accurate treatment of excited states such as the  $GW$  approximation is expected to raise band gaps by  $\sim 1.5$  eV in this pressure range [7,10]. A similar and opposite effect is expected to arise from the treatment of nuclear quantum effects [46–50]. These opposite effects likely happen to cancel out to a large degree,

which is likely responsible for the close agreements between the computed and measured direct gap and transition pressure values reported in our previous work [29].

The phonon dispersion relations of the  $C2/c-24$  phase at 500 GPa both in the harmonic and anharmonic approximations are presented in Fig. 2. We observe that the anharmonic corrections increase the lower phonon frequencies, which correspond to collective motion of the atoms within a plane, while they decrease the higher phonon frequencies which correspond to intramolecular vibrations (vibrons). The Eliashberg function ( $\alpha^2F$ ) and the phonon densities of states (PhDOS) are also presented in Fig. 2. The  $\alpha^2F$  and PhDOS are qualitatively similar, indicating that the electron-phonon coupling is not provided by specific phonon modes. We also show the electron-phonon coupling parameter defined as  $\lambda(\omega) = \int_0^\omega \frac{d\omega'}{\omega'} \alpha^2F(\omega')$  in Fig. 2. Although the overall shape of  $\lambda(\omega)$  in the harmonic and anharmonic cases are similar, the anharmonic values are smaller because the lower phonon frequencies are pushed up and the integral includes the frequency in the denominator. The electron-phonon coupling constant  $\lambda$  corresponds to  $\lambda(\infty)$  and is equal to 1.80 and 1.53 for the harmonic and anharmonic cases, respectively. The analogous plots for 400 and 450 GPa are presented in Fig. S4 and Fig. S5, respectively, and can be interpreted in the same way.

The resulting values of the superconducting transition temperatures ( $T_c$ ) using the Allen-Dynes formula [51] ( $\mu^* = 0.1$ ) are reported in Table I. We see that the  $T_c$  values for harmonic and anharmonic cases are close despite the fact that  $\lambda$  reduces significantly when anharmonic effects are included. This is due to the fact that  $\omega_{\log}$  values for the anharmonic calculations are significantly higher, and the two effects mostly cancel out. We note that we use a standard value of 0.1 for the semiempirical Coulomb pseudopotential to arrive at these  $T_c$  values. First-principles estimations of this parameter vary between 0.08 and 0.16 for hydrogen in the  $Cmca-4$  phase [52]. For example, using the ends of this interval would yield an Allen-Dynes  $T_c$  between 147 and 201 K at 500 GPa.

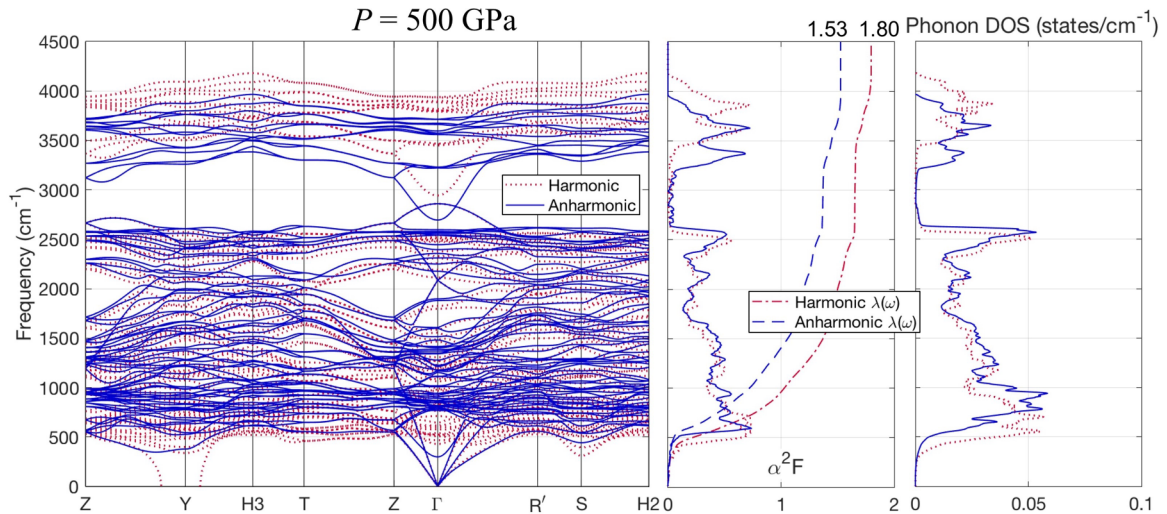


FIG. 2. Phonons and electron-phonon coupling at 500 GPa. The phonon dispersion relations for the C2/c-24 phase of hydrogen at 500-GPa pressure (left panel). The harmonic and anharmonic calculations are shown by red dashed lines and blue solid lines, respectively. The Eliashberg function  $\alpha^2F$  and the electron-phonon coupling parameter  $\lambda(\omega)$  (middle panel), and the phonon densities of states (right panel).

It has been shown that in the case of high anisotropy in electron-phonon coupling in the  $k$  space, superconducting properties are not captured accurately by the isotropic Eliashberg theory [45,53]. However, the computational cost of anisotropic Eliashberg calculations is very high, and isotropic calculations are preferred when possible. To check the degree of anisotropy in the  $k$  space, we plot the band- and  $k$ -point resolved electron-phonon coupling ( $\lambda_{n,k}$ ) in Fig. 3(a) for 500 GPa in the anharmonic approximation. We find that  $\lambda_{n,k}$  is mostly isotropic, with some anisotropy in the hole pockets (band 2). The analogous plot for the harmonic case is presented in Fig. S6. We then proceed to the isotropic Eliashberg calculations to determine leading edge of the superconducting gap ( $\Delta_0$ ) vs temperature, which is shown in Fig. 3(b) for all the computed pressures in the harmonic and anharmonic approximations. The  $T_c$  values obtained from these calculations are also reported in Table I. The rapid increase of  $T_c$  with pressure can largely be explained by the rapid increase of the electronic density of states at the Fermi level.

We find that the expected  $T_c$  at the 500 GPa (242 K) is very high and comparable to the predicted  $T_c$  of the Cmca-4 phase at 450 GPa (258 K) [54]. In contrast to the previous work on the Cmca-4 phase [54], anharmonicity does not greatly enhance superconductivity in the C2/c-24 but instead very slightly diminishes it. We note that the inclusion of nuclear

quantum effects and a better treatment of electron self-energy effects (such as the  $GW$  method) would change these reported values, especially if these effects occur in substantially nonuniform ways in the reciprocal space. However, we do not think this is likely, since the electronic and vibrational structure we base these calculations on are consistent with the experimental measurements [29]. It is more likely that the opposite effects of the quantum behavior of the nuclei and electron self-energy are largely uniform and similar in size, and the overall qualitative picture, i.e., that  $T_c$  rapidly increases in the 400–500-GPa range from  $<10$  K to  $>200$  K, is a robust result. We also note that recently a parameter based on the electron localization function (ELF) was proposed as highly correlated with  $T_c$  in hydrides [55]. This parameter, called the networking value ( $\phi$ ), corresponds to the largest value of ELF for which the isosurface of ELF creates a connected network in all three directions. For the C2/c-24 phase, we find  $\phi$  to be 0.271, 0.275, and 0.276 at 400, 450, and 500 GPa, respectively. In Fig. S1, we present the plot of the ELF isosurface at the value  $\phi = 0.276$  for 500 GPa. Finally, in order to provide another theoretical datapoint for experimental studies that may measure optical properties of high-pressure hydrogen samples, we present the dielectric function and reflectivity of the C2/c-24 phase 500 GPa calculated in the random-phase approximation in Fig. S7.

TABLE I. Electron-phonon coupling constant and  $T_c$ . The electron-phonon coupling constant  $\lambda$  and the superconducting transition temperature  $T_c$  using both the Allen-Dynes formula and the isotropic Eliashberg theory are shown in the harmonic and anharmonic cases for 400, 450, and 500 GPa. The Coulomb pseudopotential is set to 0.1 in all cases.

$P$ (GPa)	$\lambda$		$T_c$ (Allen-Dynes) (K)		$T_c$ (Eliashberg) (K)	
	Harmonic	Anharmonic	Harmonic	Anharmonic	Harmonic	Anharmonic
400	0.43	0.32	8.5	1.6	8.5	1.6
450	0.95	0.82	79	83	100	94
500	1.80	1.53	186	190	245	242



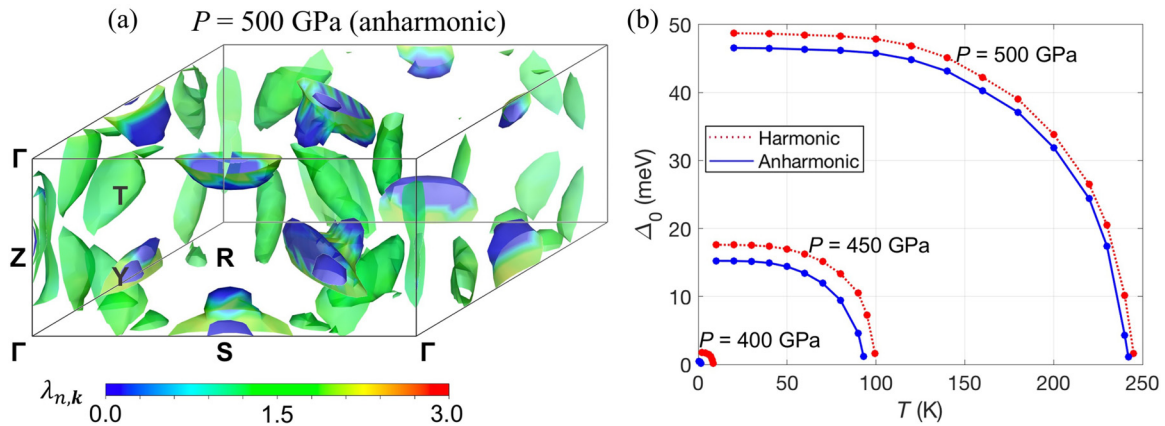


FIG. 3. Electron-phonon coupling and superconducting gap. (a) Band- and  $k$ -point resolved electron-phonon coupling for 500 GPa for the  $C2/c-24$  phase of hydrogen in the anharmonic approximation shown in the reciprocal space. (b) Leading edge of the superconducting gap vs temperature for 400, 450, and 500 GPa in the harmonic and anharmonic approximations.

In summary, we have found that the predicted superconducting transition temperatures for the  $C2/c-24$  phase at 400, 450, and 500 GPa are 1.6, 94, and 242 K, respectively. The rapid rise of  $T_c$  with pressure can be understood by the transition of the material from semimetal to metal in that pressure range, as we detailed in our previous work [29]. We find that anharmonic corrections significantly change the electron-phonon coupling, but their overall impact on the superconducting properties and  $T_c$  is small. Given that the  $C2/c-24$  phase may be stable up to the transition to the atomic phase at a higher pressure around 500 GPa, we hope that our work will motivate experimental researchers to investigate the superconducting properties of hydrogen in the 400–500-GPa range. Such experiments could bring us closer to resolving one of the outstanding questions in physics, which is to understand the high-pressure properties of the simplest and the most common material in nature.

This work was supported primarily by the Director, Office of Science, Office of Basic Energy Sciences, Materials

Sciences and Engineering Division, of the U.S. Department of Energy under Contract No. DE-AC02-05-CH11231, within the Theory of Materials Program No. KC2301, which supported the structure optimization and calculation of vibrational properties. Further support was provided by the National Science Foundation (NSF) Grant No. DMR-1926004, which supported the determination of electron-phonon interactions. Computational resources used were Cori at National Energy Research Scientific Computing Center (NERSC), which is supported by the Office of Science of the U.S. Department of Energy under Contract No. DE-AC02-05-CH11231, Stampede2 at the Texas Advanced Computing Center (TACC) through Extreme Science and Engineering Discovery Environment (XSEDE), which is supported by the NSF under Grant No. ACI-1053575, Frontera at TACC, which is supported by NSF Grant No. OAC-1818253, and Bridges-2 at the Pittsburgh Supercomputing Center (PSC), which is supported by NSF Award No. ACI-1928147. We thank Hyungjun Lee for technical assistance with the EPW code.

- [1] E. Wigner and H. B. Huntington, On the possibility of a metallic modification of hydrogen, *J. Chem. Phys.* **3**, 764 (1935).
- [2] N. W. Ashcroft, Metallic hydrogen: A High-Temperature Superconductor?, *Phys. Rev. Lett.* **21**, 1748 (1968).
- [3] K. A. Johnson and N. W. Ashcroft, Structure and bandgap closure in dense hydrogen, *Nature (London)* **403**, 632 (2000).
- [4] M. Städele and R. M. Martin, Metallization of Molecular Hydrogen: Predictions from Exact-Exchange Calculations, *Phys. Rev. Lett.* **84**, 6070 (2000).
- [5] C. J. Pickard and R. J. Needs, Structure of Phase III of solid hydrogen, *Nat. Phys.* **3**, 473 (2007).
- [6] P. Cudazzo, G. Profeta, A. Sanna, A. Floris, A. Continenza, S. Massidda, and E. K. U. Gross, Ab Initio Description of High-Temperature Superconductivity in Dense Molecular Hydrogen, *Phys. Rev. Lett.* **100**, 257001 (2008).
- [7] S. Lebègue, C. M. Araujo, D. Y. Kim, M. Ramzan, H. Mao, and R. Ahuja, Semimetallic dense hydrogen above 260 GPa, *Proc. Natl Acad. Sci. USA* **109**, 9766 (2012).
- [8] C. J. Pickard, M. Martinez-Canales, and R. J. Needs, Density functional theory study of Phase IV of solid hydrogen, *Phys. Rev. B* **85**, 214114 (2012).
- [9] M. A. Morales, J. M. McMahon, C. Pierleoni, and D. M. Ceperley, Towards a predictive first-principles description of solid molecular hydrogen with density functional theory, *Phys. Rev. B* **87**, 184107 (2013).
- [10] J. McMinis, R. C. Clay, D. Lee, and M. A. Morales, Molecular to Atomic Phase Transition in Hydrogen under High Pressure, *Phys. Rev. Lett.* **114**, 105305 (2015).
- [11] N. D. Drummond, B. Monserrat, J. H. Lloyd-Williams, P. L. Ríos, C. J. Pickard, and R. J. Needs, Quantum Monte Carlo study of the phase diagram of solid molecular hydrogen at extreme pressures, *Nat. Commun.* **6**, 7794 (2015).
- [12] B. Monserrat, R. J. Needs, E. Gregoryanz, and C. J. Pickard, Hexagonal structure of Phase III of solid hydrogen, *Phys. Rev. B* **94**, 134101 (2016).

- [13] S. Azadi, N. D. Drummond, and W. M. C. Foulkes, Nature of the metallization transition in solid hydrogen, *Phys. Rev. B* **95**, 035142 (2017).
- [14] B. Monserrat, N. D. Drummond, P. Dalladay-Simpson, R. T. Howie, P. López Ríos, E. Gregoryanz, C. J. Pickard, and R. J. Needs, Structure and Metallicity of Phase V of Hydrogen, *Phys. Rev. Lett.* **120**, 255701 (2018).
- [15] X.-W. Zhang, E.-G. Wang, and X.-Z. Li, Ab initio investigation on the experimental observation of metallic hydrogen, *Phys. Rev. B* **98**, 134110 (2018).
- [16] C. Zhang, C. Zhang, M. Chen, W. Kang, Z. Gu, J. Zhao, C. Liu, C. Sun, and P. Zhang, Finite-temperature infrared and Raman spectra of high-pressure hydrogen from first-principles molecular dynamics, *Phys. Rev. B* **98**, 144301 (2018).
- [17] P. Loubeyre, F. Occelli, and R. LeToullec, Optical studies of solid hydrogen to 320 GPa and evidence for black hydrogen, *Nature (London)* **416**, 613 (2002).
- [18] R. T. Howie, C. L. Guillaume, T. Scheler, A. F. Goncharov, and E. Gregoryanz, Mixed Molecular and Atomic Phase of Dense Hydrogen, *Phys. Rev. Lett.* **108**, 125501 (2012).
- [19] M. I. Eremets, I. A. Troyan, P. Lerch, and A. Drozdov, Infrared study of hydrogen up to 310 GPa at Room temperature, *High Pressure Res.* **33**, 377 (2013).
- [20] P. Loubeyre, F. Occelli, and P. Dumas, Hydrogen Phase IV revisited via synchrotron infrared measurements in H<sub>2</sub> and D<sub>2</sub> up to 290 GPa at 296 K, *Phys. Rev. B* **87**, 134101 (2013).
- [21] R. P. Dias, O. Noked, and I. F. Silvera, Quantum phase transition in solid hydrogen at high pressure, *Phys. Rev. B* **100**, 184112 (2019).
- [22] M. I. Eremets, A. P. Drozdov, P. P. Kong, and H. Wang, Semimetallic molecular hydrogen at pressure above 350 GPa, *Nat. Phys.* **15**, 1246 (2019).
- [23] P. Loubeyre, F. Occelli, and P. Dumas, Synchrotron infrared spectroscopic evidence of the probable transition to metal hydrogen, *Nature (London)* **577**, 631 (2020).
- [24] P. Loubeyre, F. Occelli, and P. Dumas, Comment on: Observation of the Wigner-Huntington transition to metallic hydrogen, [arXiv:1702.07192](https://arxiv.org/abs/1702.07192).
- [25] M. I. Eremets and A. P. Drozdov, Comments on the claimed observation of the Wigner-Huntington transition to metallic hydrogen, [arXiv:1702.05125](https://arxiv.org/abs/1702.05125).
- [26] I. F. Silvera and R. Dias, Comment on: Observation of a first order phase transition to metal hydrogen near 425 GPa, [arXiv:1907.03198](https://arxiv.org/abs/1907.03198).
- [27] R. P. Dias and I. F. Silvera, Observation of the Wigner-Huntington transition to metallic hydrogen, *Science* **355**, 715 (2017).
- [28] I. F. Silvera and R. Dias, Metallic hydrogen, *J. Phys.: Condens. Matter* **30**, 254003 (2018).
- [29] M. Dogan, S. Oh, and M. L. Cohen, Observed metallization of hydrogen interpreted as a band structure Effect, *J. Phys.: Condens. Matter* **33**, 03LT01 (2020).
- [30] A. P. Drozdov, M. I. Eremets, I. A. Troyan, V. Ksenofontov, and S. I. Shylin, Conventional superconductivity at 203 Kelvin at high pressures in the sulfur hydride system, *Nature (London)* **525**, 73 (2015).
- [31] M. Somayazulu, M. Ahart, A. K. Mishra, Z. M. Geballe, M. Baldini, Y. Meng, V. V. Struzhkin, and R. J. Hemley, Evidence for Superconductivity above 260 K in Lanthanum Superhydride at Megabar Pressures, *Phys. Rev. Lett.* **122**, 027001 (2019).
- [32] A. P. Drozdov, P. P. Kong, V. S. Minkov, S. P. Besedin, M. A. Kuzovnikov, S. Mozaffari, L. Balicas, F. F. Balakirev, D. E. Graf, V. B. Prakapenka, E. Greenberg, D. A. Knyazev, M. Tkacz, and M. I. Eremets, Superconductivity at 250 K in lanthanum hydride under high pressures, *Nature (London)* **569**, 528 (2019).
- [33] E. Snider, N. Dasenbrock-Gammon, R. McBride, M. Debessai, H. Vindana, K. Vencatasamy, K. V. Lawler, A. Salamat, and R. P. Dias, Room-temperature superconductivity in a carbonaceous sulfur hydride, *Nature (London)* **586**, 373 (2020).
- [34] M. Dogan and M. L. Cohen, Anomalous behavior in high-pressure carbonaceous sulfur hydride, *Physica C (Amsterdam, Neth.)* **583**, 1353851 (2021).
- [35] See Supplemental Material at <http://link.aps.org/supplemental/10.1103/PhysRevB.105.L020509> for details on the computational methods and eight supplemental figures (S1) Atomic structure and ELF isosurface taken at the networking value 0.276 (S2–S3) Fermi surfaces and band structures at 400 and 450 GPa, (S4–S5) Phonons and electron-phonon coupling at 400 GPa, (S6) Electron-phonon coupling in k-space for 500 GPa (harmonic), (S7) Dielectric function and reflectivity at 500 GPa and (S8) Original and Wannier-interpolated band structure at 400 GPa.
- [36] J. P. Perdew and A. Zunger, Self-interaction correction to density-functional approximations for many-electron systems, *Phys. Rev. B* **23**, 5048 (1981).
- [37] P. Giannozzi, S. Baroni, N. Bonini, M. Calandra, R. Car, C. Cavazzoni, Davide Ceresoli, G. L. Chiarotti, M. Cococcioni, I. Dabo, A. D. Corso, S. de Gironcoli, S. Fabris, G. Fratesi, R. Gebauer, U. Gerstmann, C. Gougoussis, Anton Kokalj, M. Lazzeri, L. Martin-Samos, N. Marzari, F. Mauri, R. Mazzarello, Stefano Paolini, A. Pasquarello, L. Paulatto, C. Sbraccia, S. Scandolo, G. Sclauzero, A. P. Seitsonen, A. Smogunov, P. Umari, and R. M. Wentzcovitch, QUANTUM ESPRESSO: A modular and open-source software project for quantum simulations of materials, *J. Phys.: Condens. Matter* **21**, 395502 (2009).
- [38] D. R. Hamann, Optimized norm-conserving Vanderbilt pseudopotentials, *Phys. Rev. B* **88**, 085117 (2013).
- [39] A. Kokalj, Computer graphics and graphical user interfaces as tools in simulations of matter at the atomic scale, *Comput. Mater. Sci.* **28**, 155 (2003).
- [40] X. Gonze and C. Lee, Dynamical matrices, born effective charges, dielectric permittivity tensors, and interatomic force constants from density-functional perturbation theory, *Phys. Rev. B* **55**, 10355 (1997).
- [41] S. Baroni, S. de Gironcoli, A. Dal Corso, and P. Giannozzi, Phonons and related crystal properties from density-functional perturbation theory, *Rev. Mod. Phys.* **73**, 515 (2001).
- [42] M. L. Cohen, M. Schlüter, J. R. Chelikowsky, and S. G. Louie, Self-consistent pseudopotential method for localized configurations: Molecules, *Phys. Rev. B* **12**, 5575 (1975).
- [43] T. Tadano, Y. Gohda, and S. Tsuneyuki, Anharmonic force constants extracted from first-principles molecular dynamics: Applications to heat transfer simulations, *J. Phys.: Condens. Matter* **26**, 225402 (2014).

- [44] T. Tadano and S. Tsuneyuki, Self-consistent phonon calculations of lattice dynamical properties in cubic SrTiO<sub>3</sub> with first-principles anharmonic force constants, *Phys. Rev. B* **92**, 054301 (2015).
- [45] S. Ponc e, E. R. Margine, C. Verdi, and F. Giustino, EPW: Electron-phonon coupling, transport and superconducting properties using maximally localized Wannier functions, *Comput. Phys. Commun.* **209**, 116 (2016).
- [46] X.-Z. Li, B. Walker, M. I. J. Probert, C. J. Pickard, R. J. Needs, and A. Michaelides, Classical and quantum ordering of protons in cold solid hydrogen under megabar pressures, *J. Phys.: Condens. Matter* **25**, 085402 (2013).
- [47] M. A. Morales, J. M. McMahon, C. Pierleoni, and D. M. Ceperley, Nuclear Quantum Effects and Nonlocal Exchange-Correlation Functionals Applied to Liquid Hydrogen at High Pressure, *Phys. Rev. Lett.* **110**, 065702 (2013).
- [48] S. Azadi, R. Singh, and T. D. K uhne, Nuclear quantum effects induce metallization of dense solid molecular hydrogen, *J. Comput. Chem.* **39**, 262 (2018).
- [49] V. Gorelov, M. Holzmann, D. M. Ceperley, and C. Pierleoni, Energy Gap Closure of Crystalline Molecular Hydrogen with Pressure, *Phys. Rev. Lett.* **124**, 116401 (2020).
- [50] L. Monacelli, I. Errea, M. Calandra, and F. Mauri, Black metal hydrogen above 360 GPa driven by proton quantum fluctuations, *Nat. Phys.* **17**, 63 (2021).
- [51] P. B. Allen and R. C. Dynes, Transition temperature of strongly-coupled superconductors reanalyzed, *Phys. Rev. B* **12**, 905 (1975).
- [52] P. Cudazzo, G. Profeta, A. Sanna, A. Floris, A. Continenza, S. Massidda, and E. K. U. Gross, Electron-phonon interaction and superconductivity in metallic molecular hydrogen. II. Superconductivity under pressure, *Phys. Rev. B* **81**, 134506 (2010).
- [53] H. J. Choi, D. Roundy, H. Sun, M. L. Cohen, and S. G. Louie, The origin of the anomalous superconducting properties of MgB<sub>2</sub>, *Nature (London)* **418**, 758 (2002).
- [54] M. Borinaga, P. Riego, A. Leonardo, M. Calandra, F. Mauri, A. Bergara, and I. Errea, Anharmonic enhancement of superconductivity in metallic molecular *Cmca* - 4 Hydrogen at high pressure: A first-principles study, *J. Phys.: Condens. Matter* **28**, 494001 (2016).
- [55] F. Belli, T. Novoa, J. Contreras-Garc a and I. Errea, Strong correlation between bonding network and critical temperature in hydrogen-based superconductors, *Nat. Commun.* **12**, 5381 (2021).